REPORT SAMSO-TR-76-142

(12)

Impact Damage Mechanisms of 3-D Carbon-Carbon Materials

Materials Sciences Laboratory
Laboratory Operations
The Aerospace Corporation
El Segundo, California, 90245

23 July 1976

Final Report
(1 July - 31 August 1975)

Prepared for

SPACE AND MISSILE SYSTEMS ORGANIZATION
AIR FORCE SYSTEMS COMMAND
Los Angeles Air Force Station
P.O. Box 92960, Worldway Postal Center
Los Angeles, Calif. 90009

This final report was submitted by The Aerospace Corporation, El Segundo, CA 90245, under Contract F04701-75-C-0076 with the Space and Missile Systems Organization, Deputy for Reentry Systems, P. O. Box 92960, Worldway Postal Center, Los Angeles, CA 90009. It was reviewed and approved for The Aerospace Corporation by W. C. Riley, Laboratory Operations, and R. G. Allen, Reentry Systems Division. The project officer was Capt. Don E. Jackson, SAMSO (RSSE).

This report has been reviewed by the Information Office (OI) and is releasable to the National Technical Information Service (NTIS). At NTIS, it will be available to the general public, including foreign nations.

This technical report has been reviewed and is approved for publication. Publication of this report does not constitute Air Force approval of the report's findings or conclusions. It is published only for the exchange and stimulation of ideas.

Don E. Jackson

Don E. Jackson, Capt, USAF
Aeromechanics and Materials Division
Directorate of Ballistic Systems
Deputy for Reentry Systems

William Goldberg, Lt Col, USAF
Chief, Aeromechanics and Materials Division
Directorate of Ballistic Systems
Deputy for Reentry Systems

FOR THE COMMANDER

Donald A. Dowler

Donald A. Dowler, Col, USAF
Director, Ballistic Systems
Deputy for Reentry Systems

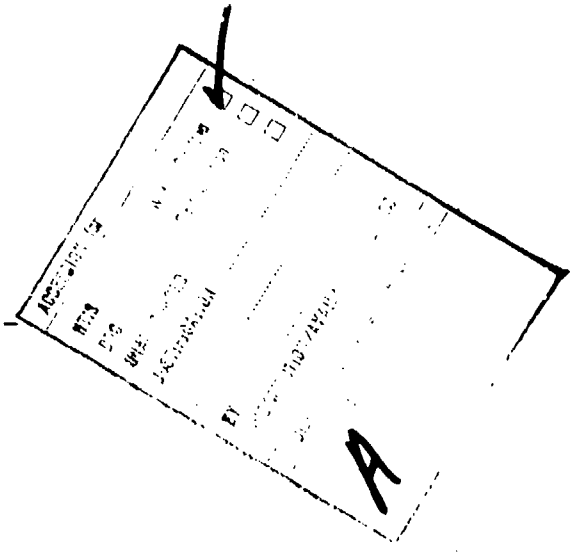

UNCLASSIFIED

SECURITY CLASSIFICATION OF THIS PAGE (When Data Entered)

REPORT DOCUMENTATION PAGE

READ INSTRUCTIONS BEFORE COMPLETING FORM

1. REPORT NUMBER: SAMSO-TR-76-142	2. GOVT ACCESSION NO.
3. RECIPIENT'S CATALOG NUMBER	
4. TITLE (and Subtitle): IMPACT DAMAGE MECHANISMS OF 3-D CARBON-CARBON MATERIAL.	5. TYPE OF REPORT & PERIOD COVERED: Final rept. 1 Jul–31 Aug 75
6. PERFORMING ORG. REPORT NUMBER: TR-0076(6550-77)-2	
7. AUTHOR(s): Louis Rubin	8. CONTRACT OR GRANT NUMBER(s): F04701-75-C-0076
9. PERFORMING ORGANIZATION NAME AND ADDRESS: The Aerospace Corporation, El Segundo, CA 90245	10. PROGRAM ELEMENT, PROJECT, TASK AREA & WORK UNIT NUMBERS
11. CONTROLLING OFFICE NAME AND ADDRESS: Space and Missile Systems Organization, Air Force Systems Command, Los Angeles, CA 90009	12. REPORT DATE: 23 July 1976
	13. NUMBER OF PAGES: 24
14. MONITORING AGENCY NAME & ADDRESS (if different from Controlling Office): 12 24 p.	15. SECURITY CLASS. (of this report): Unclassified
	15a. DECLASSIFICATION/DOWNGRADING SCHEDULE

16. DISTRIBUTION STATEMENT (of this Report)

Approved for public release; distribution unlimited.

17. DISTRIBUTION STATEMENT (of the abstract entered in Block 20, if different from Report)

18. SUPPLEMENTARY NOTES

19. KEY WORDS (Continue on reverse side if necessary and identify by block number)

Erosion
Carbon-Carbon
Microstructure
Hydrometeor Erosion
Nosetip Materials

20. ABSTRACT (Continue on reverse side if necessary and identify by block number)

Impact-induced damage mechanisms for GE 2-2-3 Carbon-Carbon have been identified for both axial and transverse fiber bundles, and changes in the nature and severity of damage have been observed as a function of location with respect to the impact crater geometry. Although axial fiber bundles exhibited column buckling failure when immediately beneath an impact crater, they were relatively intact (except for tensile cracks in some individual fibers) at positions alongside or away from the major craters. Transverse fiber

DD FORM 1473 (FACSIMILE)

UNCLASSIFIED

SECURITY CLASSIFICATION OF THIS PAGE (When Data Entered)

403 644

19. KEY WORDS (Continued)

20. ABSTRACT (Continued)

bundles, however, showed column buckling failure in locations alongside or between craters, while only flexural-type failures were noted in locations directly below a crater.

CONTENTS

FIGURES

PREFACE

This report covers work done for the Reentry Systems Division by the Materials Sciences Laboratory of The Aerospace Corporation, El Segundo, California, under Air Force Space and Missile Systems Organization (SAMSO) Contract No. F04701-75-C-0076.

The author wishes to thank A. DiGiacomo, G. Henderson, and A. Palyo for their valuable assistance in sample preparation and scanning electron microscopy.

I. INTRODUCTION

An understanding of the response of a material to an erosion environment requires a knowledge of the mechanisms by which the structural integrity is degraded and mass loss takes place. This type of information can best be derived by detailed microstructural examinations of recovered post-test specimens. In order to illustrate the type of insight obtainable and to provide additional background information for evaluation of the current SAMSO baseline material, General Electric 2-2-3 Carbon-Carbon, a limited project was undertaken by The Aerospace Corporation's Materials Sciences Laboratory to carry out a microstructural survey of an impact-damaged test specimen of this material.

II. EXPERIMENTAL BACKGROUND

The material that was examined, GE 2-2-3 Carbon-Carbon, has an orthogonal 3-dimensional construction of Thornel 50 graphite fibers with a matrix of chemically vapor-deposited pyrolytic graphite and a graphitized pitch. The Thornel 50 yarns are arrayed so that a unit cell of the composite contains 2 yarns each in the X and Y (transverse) directions and 3 yarns in the Z (axial) direction. Spacing between Z yarns is 0.030 in.; spacing between layers of X-Y yarns is 0.033 in.

During the course of a SAMSO test series at Science Applications, Inc., the specimen of GE 2-2-3 Carbon-Carbon was impacted at 10,000 fps by three sequential waves of multiple 500 μm-diameter glass beads to pre-damage the surface. A sequential series of single 1000 μm-diameter glass beads was then fired at the target at 10,000 fps to assess mass loss enhancement caused by the pre-damage condition. An overview of the specimen in the original, pre-damaged, and final states is shown in Figure 1; a more detailed overview of the two major craters selected for examination is shown in Figure 2.

For our examination of microstructural subsurface damage modes, the specimen was cross-sectioned through the center of two adjacent major impact craters using a diamond-coated wire saw. The cut surface was metallurgically polished and ion etched with xenon. In order to include two impact craters in our cutting plan, the cross-sectioning cut had to be made at a diagonal across the orthogonal fiber array. Consequently, this exposed alternate groups of X-Y and Z fiber bundles so that damage to both types of fibers is visible in a single view of the specimen cross-section.

III. MICROSTRUCTURAL DAMAGE SURVEY

The scanning electron microscope (SEM) was used to examine the details of subsurface damage of the carbon-carbon specimen. A view of the entire damage-affected area beneath the major craters is shown in the SEM composite photomicrograph of Figure 3. Aside from the massive fractures evident in the residual fiber bundles within the craters, there is a significant amount of subsurface damage. Scanning Figure 3 from left to right following the crater boundaries, examples of column buckling of transverse fiber bundles can be seen adjacent to and also some distance away from the side of a major crater. Axial fiber bundles intersecting the side of the crater appear relatively intact below the surface, but those Z bundles that are below the crater show a column buckling effect. The transverse fiber bundle immediately below the crater, however, shows a flexural failure of the fibers. This pattern is essentially repeated as we scan around the right-hand crater.

A closer look at the impact-induced damage may offer guidance for materials improvements and also provide some insight into the stress field distributions that influence materials response to erosion. If we first consider the impact effects on the Z fiber bundles, it can be seen from Figure 3 (Grids B-Q/4-5) that there is no subsurface damage to such fiber bundles that do not interact with a major crater. The Z fiber bundles that intersect or are adjacent to the crater side walls, as in Grids F-Q/11-12, F-L/21, and D-L/35-37, also show no significant in-depth damage. In areas immediately below the craters, however, there is very clear evidence of compressive loading which resulted in column buckling failure of Z bundle segments. This is illustrated in Figure 4, where localized fracture and displacement of the Z fibers (Grid J-L/14) can be seen. This type of failure is evident in that portion of the Z bundle that extends into the bottom of the crater as well as below the surface of the crater. Somewhat farther down in that fiber

bundle (Grid O-14), well below the buckled area, examples of tensile breaks in some fibers were seen and are shown in Figure 5. This type of failure would appear to result from reflected tensile waves in the specimen.

Additional examples of Z fiber fracture and displacement to yield column buckling can be seen in Figure 6. This fiber bundle (Grid J-L/19) is also at the base of the impact crater and has been subjected to high compressive loads. An enlargement of this area, Figure 7 (Grid F-L/19-21), shows that the adjacent Z fiber bundle has no apparent in-depth damage, and where it extends into the crater region, the fibers have been cleanly fractured in a mode other than compression since no fiber displacement is evident. It may be observed, however, that this entire Z fiber bundle has been bent away from the crater centerline. The relative direction of the impact forces during crater formation can thus be deduced. The fiber bundle subject to axial loading responded by a buckling failure while the adjacent fiber bundle, intersecting the crater in a side wall area, has had insufficient axial loading for buckling to occur as well as sufficient side loading to produce bending of the entire bundle.

A further illustration of this phenomenon is given in Figure 8 (Grid G-J/26-28) where, in two adjacent Z fiber bundles, the one closer to the base of the crater shows column buckling failure, while the other is relatively undamaged. The latter bundle, however, upon closer examination, does show tensile cracking in some fibers. Where buckling failure has occurred, the damage can be propagated quite a distance into the interior of the specimen. The two adjacent Z fiber bundles at the base of the crater (Grid H-O/27-29) show buckling displacement patterns extending to a distance equal to approximately one crater radius below the crater base.

The subsurface damage pattern that is evident for the transverse (X-Y) fiber bundles shows a complementary response to that observed for the axial fiber bundles. Thus, more extensive damage is seen in those areas alongside the major craters, with minimal damage shown at the base of the craters.

Figure 9 illustrates cracking and displacement of transverse fibers (Grid H/9) to provide an example of lateral column buckling. This implies a strong lateral stress path which effectively applied compressive loading to the transverse fiber bundle.

In an area at the base of a crater (Grid J-18) there is flexural failure of transverse fibers, as shown in Figure 10, but no lateral column buckling. As we reach an area between the two major craters (Grid H/24-25), buckling failure is very evident, as illustrated by the severely cracked and displaced fiber bundle segments shown in Figure 11. This failure mechanism again implies a strong transverse compressive load.

IV. SUMMARY

Impact-induced damage mechanisms for GE 2-2-3 Carbon-Carbon have been identified for both axial and transverse fiber bundles and changes in the nature and severity of damage have been observed as a function of location with respect to the impact crater geometry. Axial fiber bundles exhibited column buckling failure when immediately beneath an impact crater, but aside from some tensile cracks in individual fibers, they were relatively intact at positions alongside or away from the major craters. Transverse fiber bundles, however, showed column buckling failure in locations alongside or between craters, while only flexural-type failures were noted in locations directly below a crater.

The microstructural damage that was seen in cross-section beneath the surface of the crater sites can reasonably be assumed to represent a less severe extension of similar failure modes which, under higher stresses, resulted in catastrophic material failure and removal to form the craters. An awareness of the way in which particle impact causes a particular material to fail should prove valuable to the materials designer for the development of erosion-resistant materials. This information also serves as a tool for analytical modeling of impact response in that inputs to codes that predict failure modes at given stress levels will be based on experimental identification of actual damage mechanisms.

This limited effort was designed to show the type of information that can be derived from a microstructural examination of erosion ground or flight test materials. Such studies can range from general microstructural damage surveys to very extensive and detailed examinations, but at any level, this type of information can be of great value in understanding the erosion response of materials and offering guidelines toward the development of erosion-resistant materials.

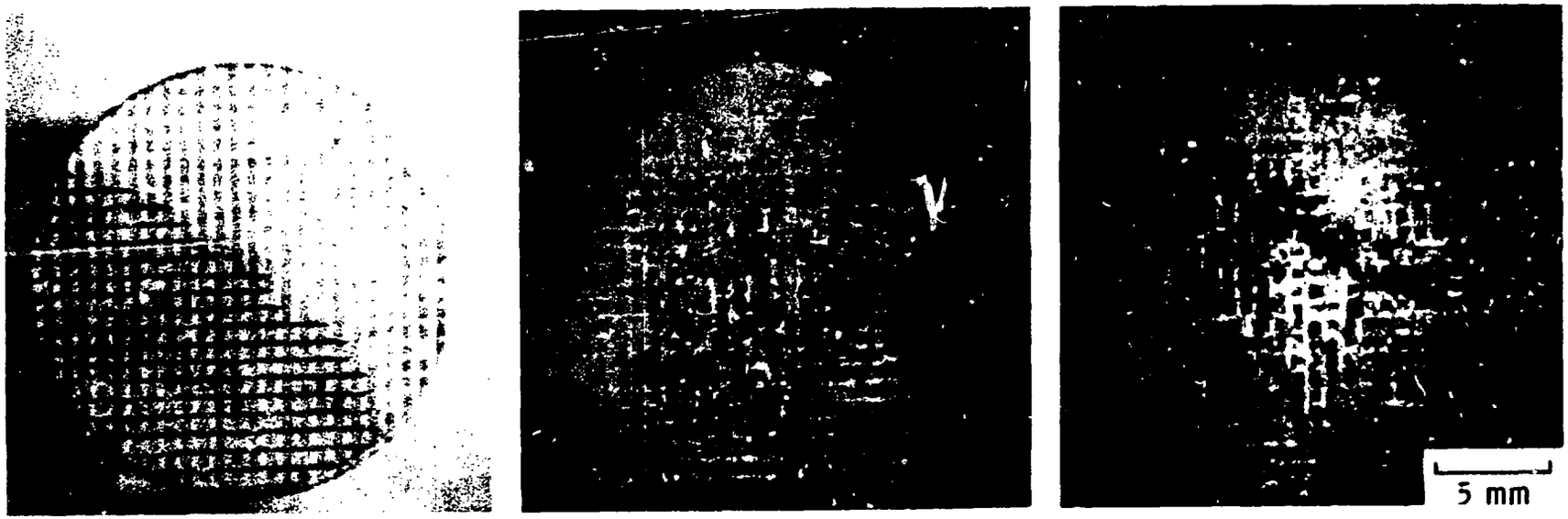

(a) ORIGINAL SPECIMEN

(b) MULTIPLE IMPACTS WITH 500 μm - DIAM GLASS BEADS

(c) SEQUENTIAL IMPACTS WITH 1000 μm - DIAM GLASS BEADS ON SPECIMEN (b)

Figure 1. Multiple Impact Sequences for GE 2-2-3 Carbon-Carbon Material

Figure 2. SEM Overview of Two Major Impact Craters

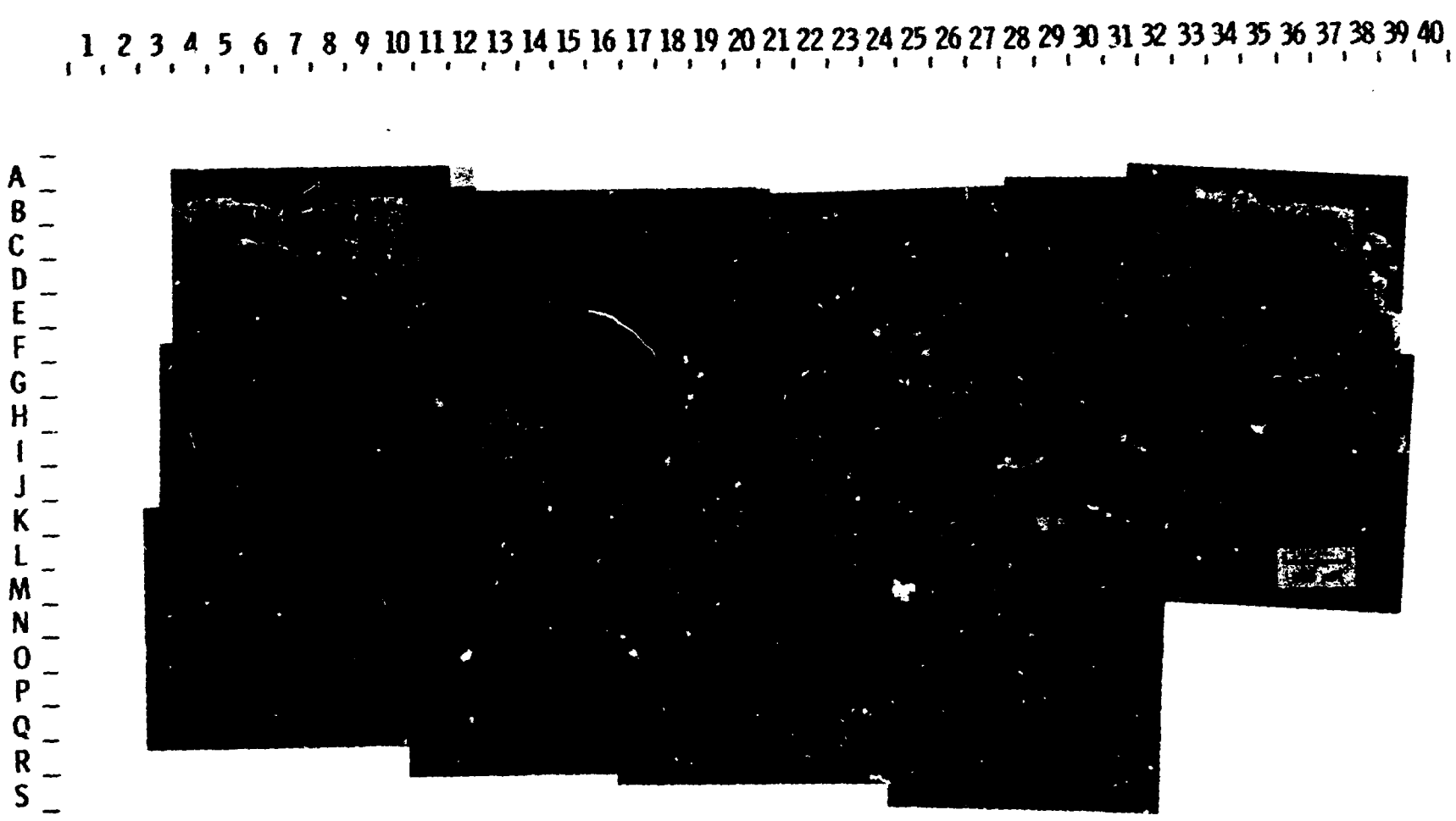

Figure 3. Cross-Section of 3-D Carbon-Carbon Specimen After Multiple Particle Impacts

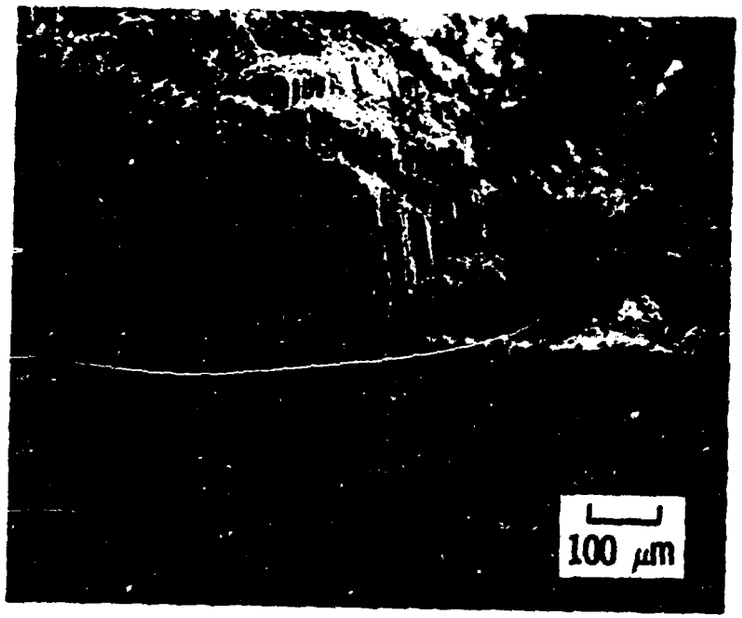

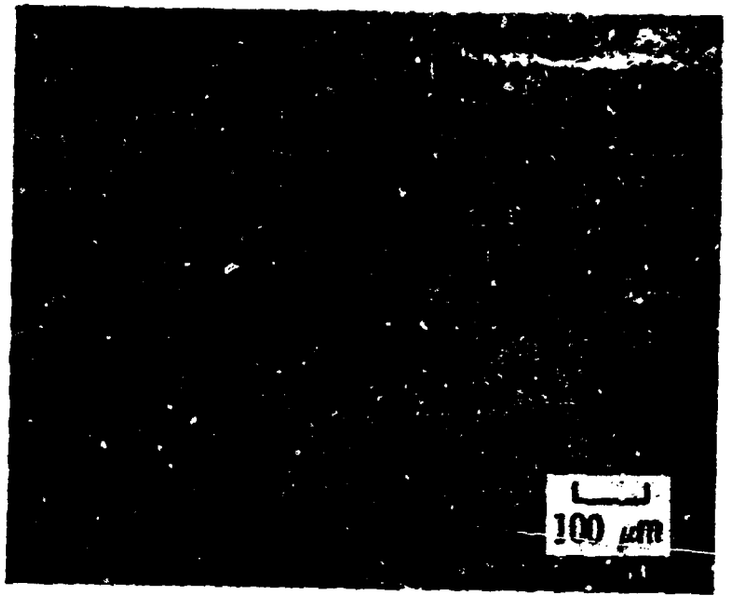

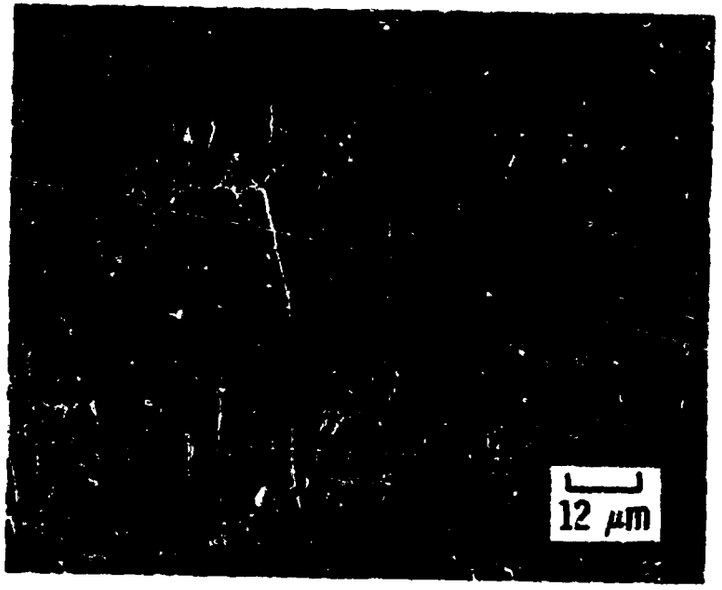

Figure 4. Details of Buckling Failure in Z Fiber Bundle

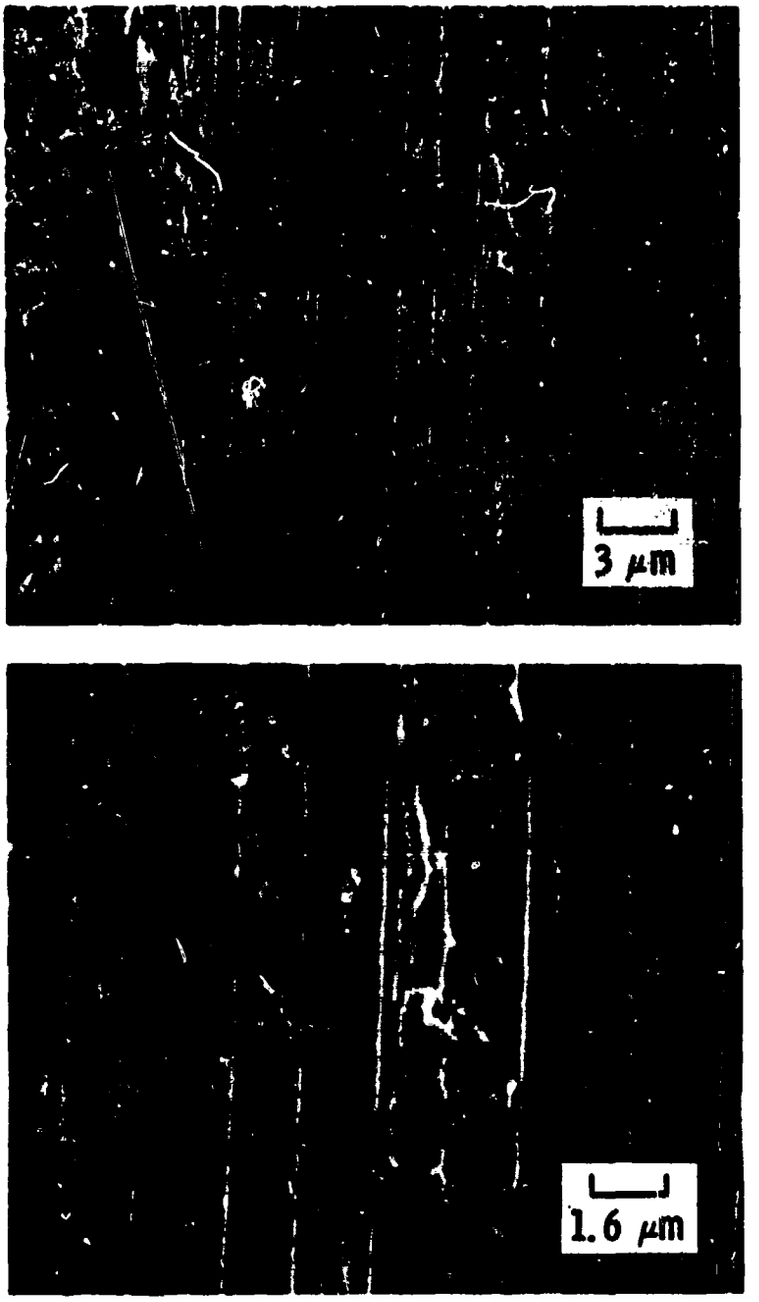

Figure 5. Localized Tensile Failure in Z Fibers

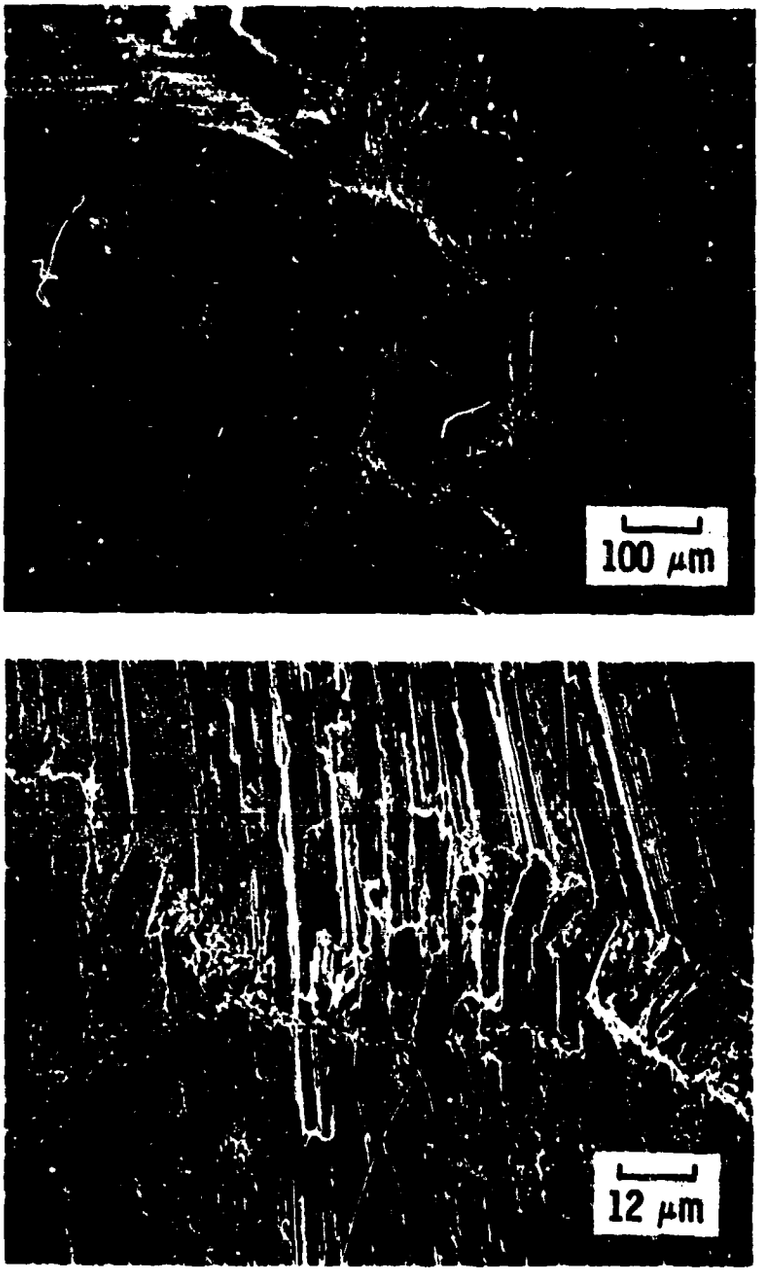

Figure 6. Z Fiber Bundle Column Buckling Failure

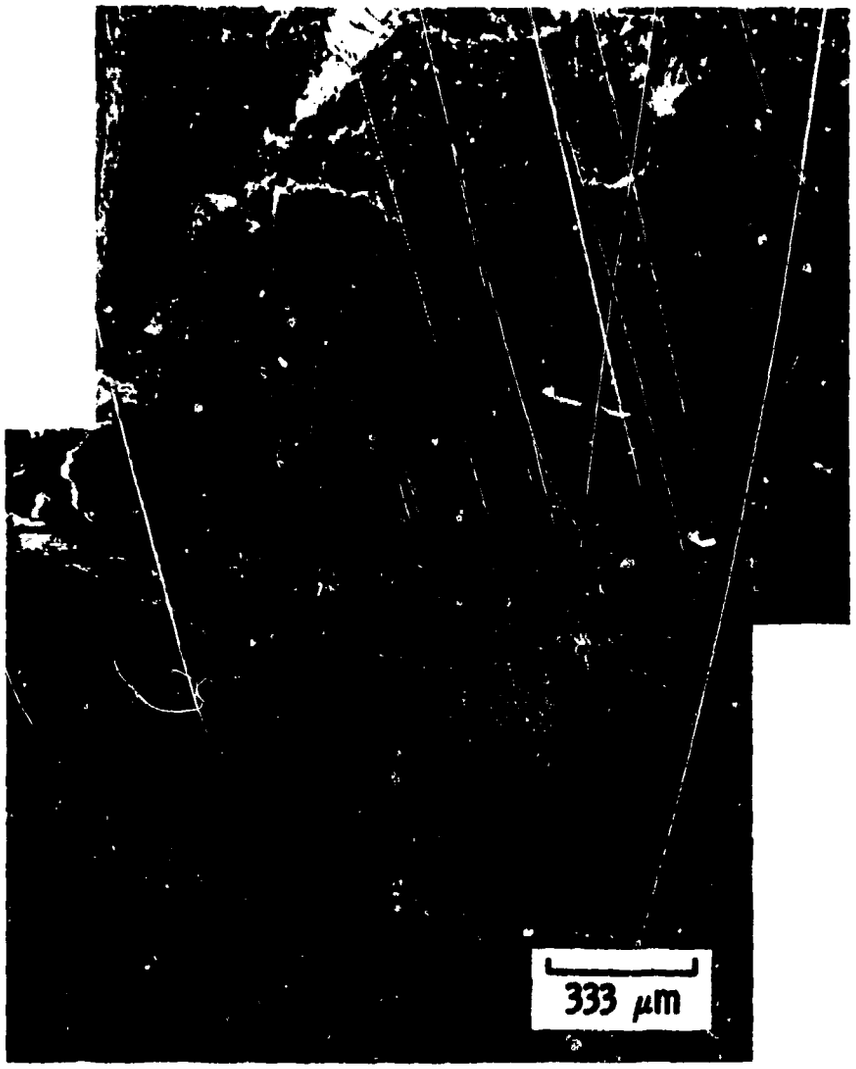

Figure 7. Z Fiber Bundles Adjacent to Major Impact Crater

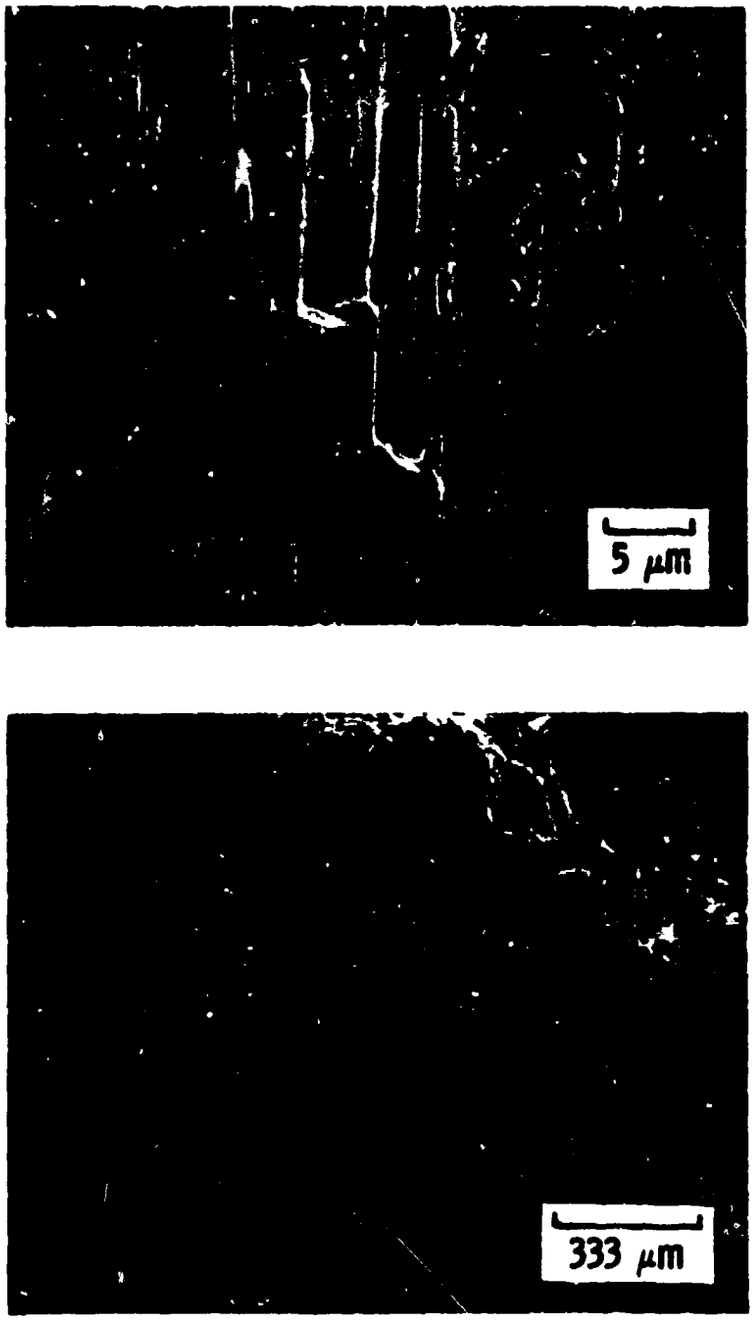

Figure 8. Tensile and Buckling Failures in Z Fiber Bundles

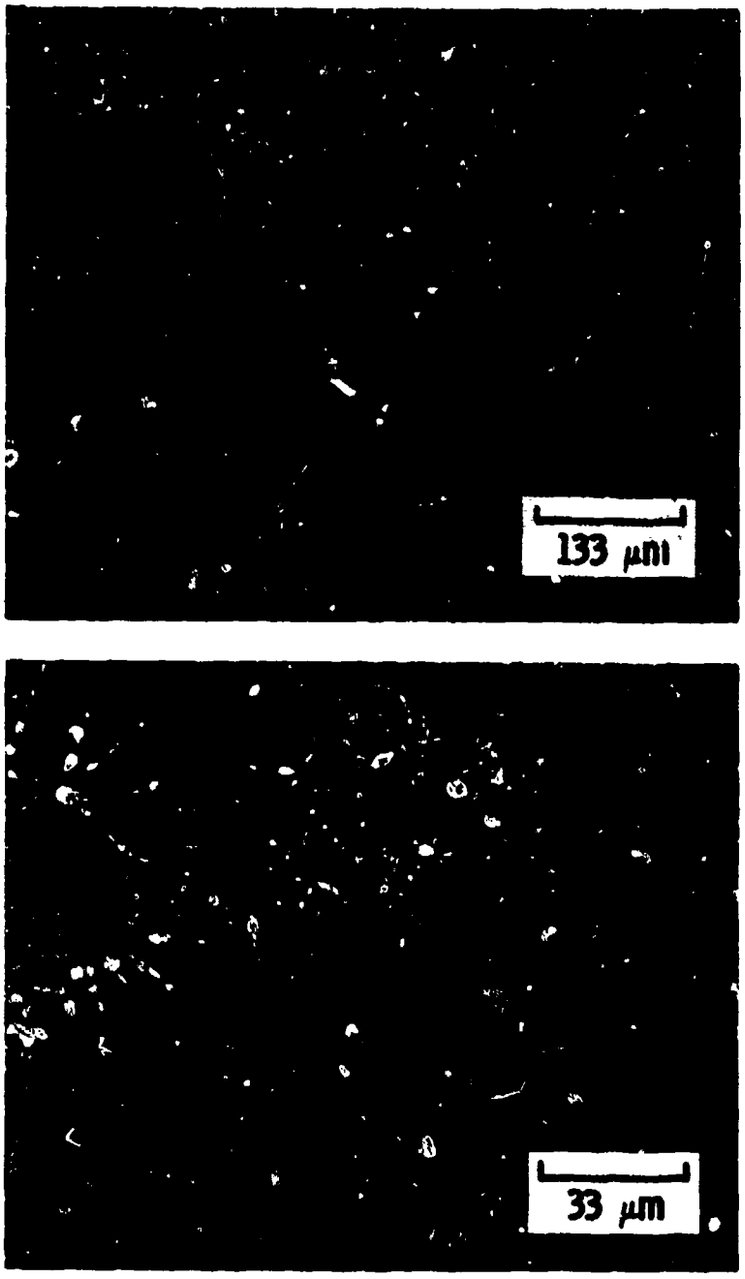

Figure 9. Column Buckling Failure in Transverse Fiber Bundle

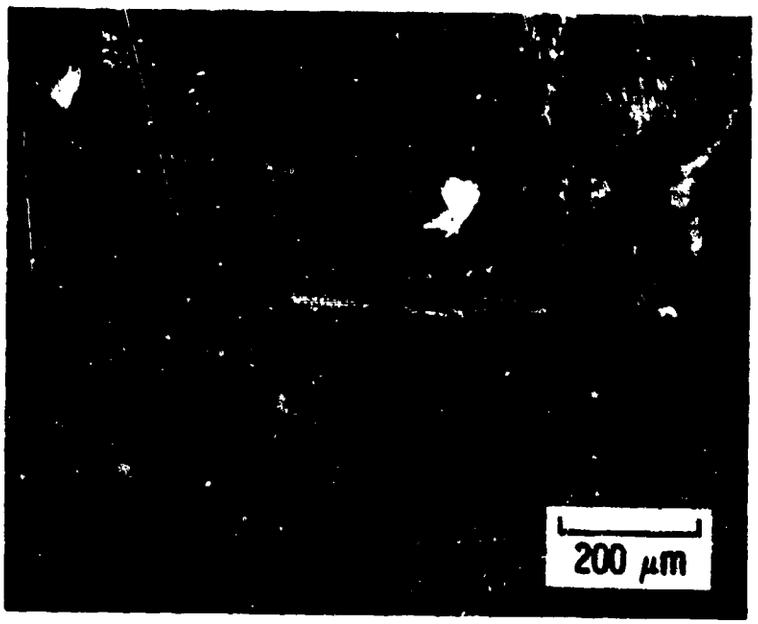

Figure 10. Flexural Failure of Transverse Fibers

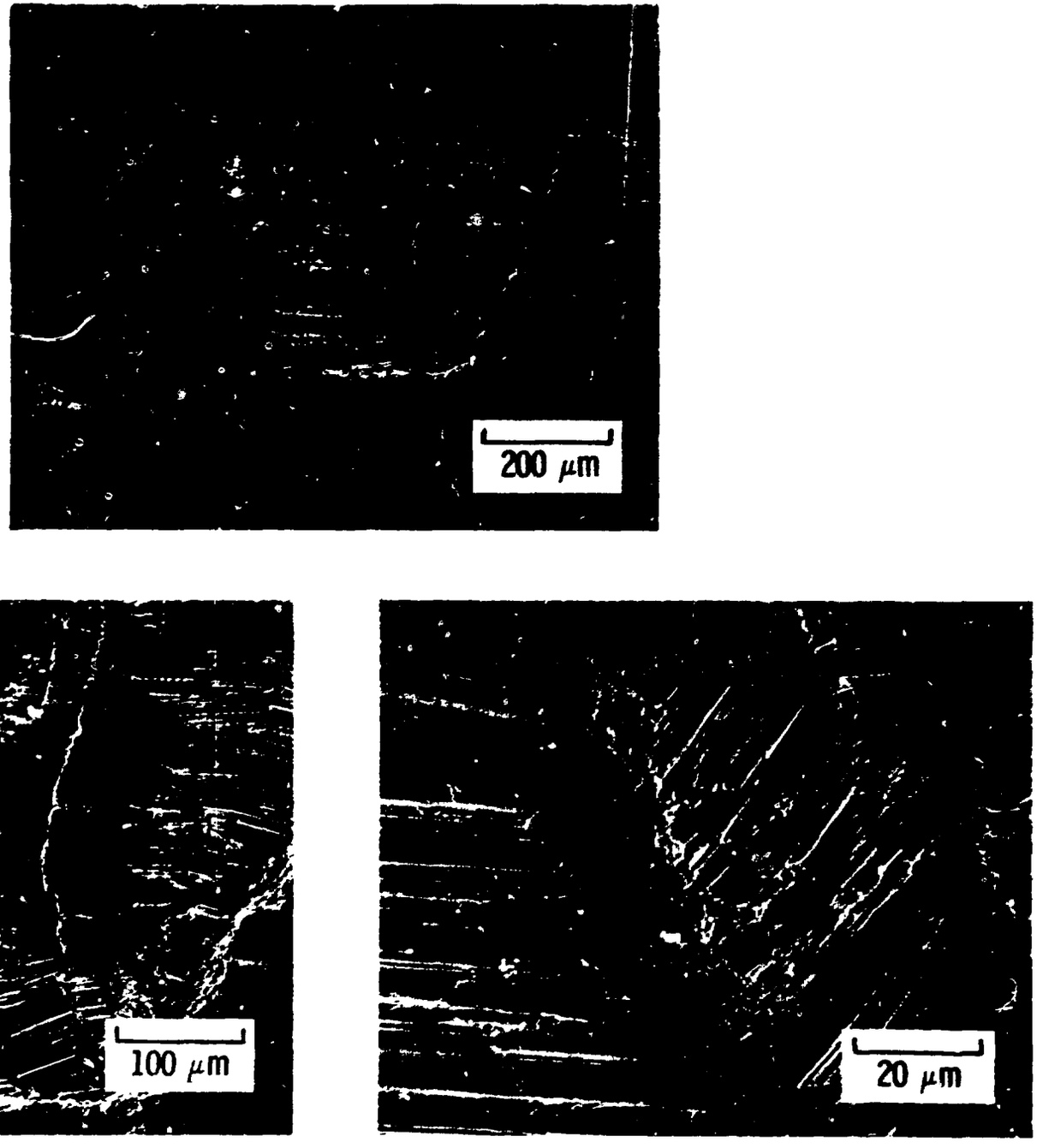

Figure 11. Detail of Column Buckling in Compressively Loaded Transverse Fiber Bundle